

Fabrication and Characterization of a Multiwall Carbon Nanotube Needle Biosensor

YeoHeung Yun^a, Adam Bange^b, Vesselin N. Shanov^c, William R. Heineman^b, H. Brian Halsall^b, Zhongyun Dong^d, Abdul Jazieh^d, Yi Tu^c, Danny Wong^f, Sarah Pixley^d, Michael Behbehani^d, Mark J. Schulz^a

^aSmart Materials Nanotechnology Laboratory, Department of Mechanical, Industrial and Nuclear Engineering,

^bDepartment of Chemistry, University of Cincinnati, Cincinnati, OH 45221

^cDepartment of Chemical and Materials Engineering, University Cincinnati, Cincinnati, OH 45221

^dCollege of Medicine, University Cincinnati, Cincinnati, OH 45221

^eFirst Nano, Inc., a Division of CVD Inc., 1860 Smithtown Ave., Ronkonkoma, NY 11779

^fDepartment of Chemistry, Macquarie University, Sydney, NSW 2109, Australia

Abstract— A nanotube electronic needle biosensor was developed to provide fast, low cost, accurate detection of biomolecules. The sensor was formed by synthesizing highly aligned multi-wall carbon nanotube arrays. Nanotube bundles from the array were welded onto the tips of tungsten needles using a microscope. The needles were then encased in glass and a polymer coating. Cyclic voltammetry (CV) for the respective reduction of 6 mM $K_3Fe(CN)_6$ in a 1.0 M KNO_3 was performed to examine the redox behavior of the nanotube needle. The CV results showed a steady-state response attributable to radial diffusion with a high steady-state current density. An amperometric sensor was then developed for glucose detection by physical attachment of glucose oxidase on the nanotube needle. A label-free immunosensor based on electrochemical impedance spectroscopy was also formed. The nanotube needle amperometric have good sensitivity with a low detection limit, and the possibility exists to keep decreasing the size of the needle to increase the sensitivity.

Keywords—Component; Multiwall Carbon Nanotube, Biosensor.

I. INTRODUCTION

Advantages of Carbon Nanotube (CNT) electrodes for biosensors include high electrical conductivity, a chemically inert electrode, high mechanical strength of a small probe, the ability to grow the nanotube array on different substrates and in different patterns, and nanoscale size of the electrode with a high aspect ratio. Different analysis methods are available for use with the electronic biosensor. The methods include electrochemical Impedance Spectroscopy (EIS) which is useful to detect non-enzymatic reactions as a label-free technique. Cyclic Voltametry and Amperometric Testing are useful to detect electro-catalytic effects and are effective ways to sense special enzyme reactions. This paper presents development of a nanotube needle biosensor starting from nanotube synthesis through to device fabrication and testing.

II. EXPERIMENTATION

Preparation of the substrate for nanotube growth is the first step in the sensor development. P-type Si wafers <100> with 4 inch diameter and a typical resistivity of 1-20 Ohm-cm are used

as substrates to grow the nanotube arrays. Some of the substrates have a 500nm SiO_2 layer on the top. Then an e-beam evaporator is used to deposit an Al thin film, and the Al is then oxidized to convert it to Al_2O_3 . Finally a catalytic iron film is deposited on the Al_2O_3 surface. The evaporation is carried out at a pressure of about 5×10^{-7} torr and the system is equipped with a film thickness monitor. The final $Fe/Al_2O_3/SiO_2/Si$ substrate is cut into 5 mm squares from one wafer where Fe is patterned on 1 mm squares to improve gas diffusion and increase the nanotube length.

Nanotube array synthesis by thermal chemical vapor deposition (CVD) is then carried out in a horizontal 2 in diameter tube furnace, the EasyTubeTM ET1000 manufactured by First Nano Inc. The nanofurnace consists of four mass flow controllers for delivery of precursor and moderator gases, a thermally driven reactor, and a vapor delivery system. Argon is used as the carrier gas to carry the water vapor to the reaction chamber. Argon is also used to purge the reactor for 20 minutes while the CVD furnace is heated to 750°C. Gas flow is then switched to ethylene, water, and hydrogen for the desired time of the deposition phase. After synthesis, the nanotube array is cooled to ambient temperature, which completes the last process step. During the cooling process, ethylene, water, and hydrogen flow is stopped and the system is purged with argon to prevent back flow of air from the exhaust line. This particular furnace has been modified by the incorporation of a quadrupole mass spectrometer sampling from the growth zone to provide more information on the growth conditions. The process conditions are: 200 SCCM of H_2 flow, 200 SCCM of C_2H_4 flow, 200 SCCM Bubbler flow, and a 750 °C growth temperature. It is assumed that all growth conditions are the same except the growth time. Various masks are sometimes used to make two-dimensional patterns on the substrate to provide different sizes and densities of nanotubes for use in the sensor.

The synthesized carbon nanotube (CNT) arrays are characterized using Environmental Scanning Electron Microscopy (ESEM) coupled with Energy Dispersive Spectroscopy (EDS), and by High Resolution Transmission Electron Microscopy (HRTEM). First, the CNT arrays are

harvested from the substrate, and dispersed in Dimethylformamide (DMF) using tip ultrasonication (Fisher) without any purification steps. HRTEM samples were prepared by placing a small droplet of the dispersion onto grids (Leci carbon support grid and Leci carbon TM grid, TED PELLA.Com) and drying in air. A JEOL JEM-2010 F TEM operated at 200 KV is used for the HRTEM imaging.

Figures 1(a-b) show ESEM results of nanotube arrays synthesized for different growth times with the assistance of water vapor. With the increase of growth time, the length of the CNT arrays increases [10]. The CNT array has high density without many impurities, which is ideal for further application development. Adhesion to the substrate is weak, and the CNT array is easily peeled off. Figure 1(a) shows one bundle of a CNT array block which is removed from the array using tweezers without damage. The CNT array is easily harvested from the substrate for use in applications. Figures 1(b) show circular posts grown on patterned arrays and the difficulty to keep the posts growing straight.

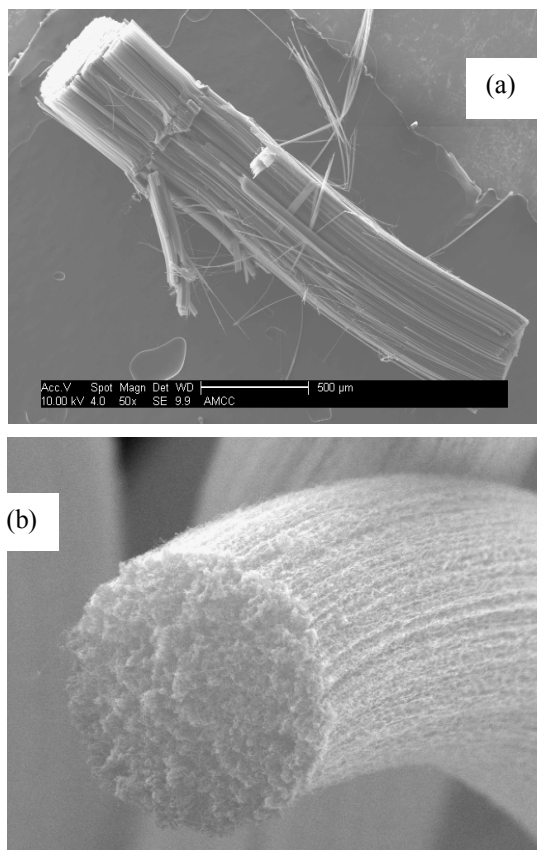


Figure 1. ESEM images of aligned MWCNT patterned arrays for 3 hours growth: (a) side view of patterned nanotube arrays; and (b) the tip of round patterned nanotube bundle 7 microns in diameter.

Welding the nanotube bundle on the tungsten needles (Goodfellow Co., Oxford, UK) was preformed with a manipulator under a bright field microscope (Fisher Scientific Inc, Micromaster 1). The tip diameter of a tungsten needle is

typically in the 1-10 µm range. A UV curing polymer (Norland optical adhesive 68) and UV lamp (Norland, 365 nm wave length) were used to electrically insulate the tungsten needles leaving only the tip of the nanotubes exposed to the analyte.

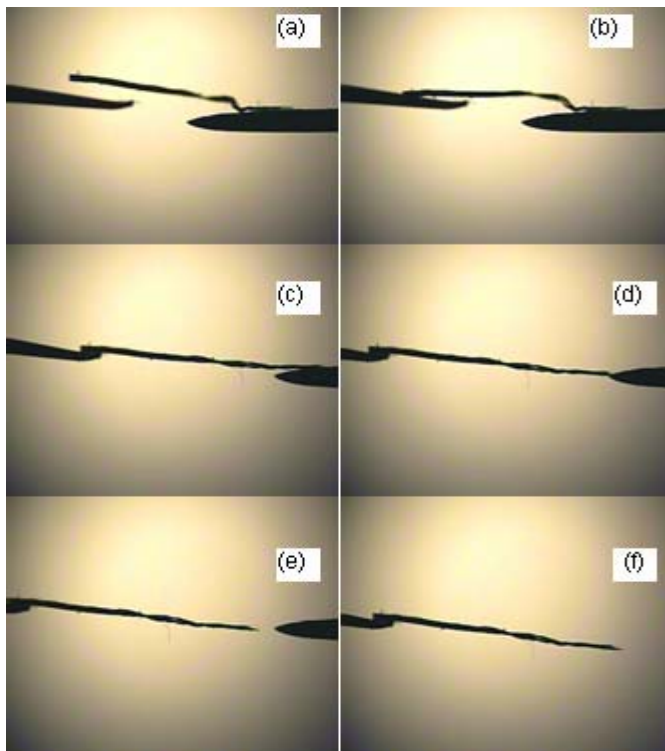


Figure 2. Welding a nanotube bundle to a tungsten tip by transferring a nanotube bundle from one tungsten tip to another in the sequence (a-f).

Figure 2 shows an approach for welding a nanotube bundle using two tungsten needles. Individual multi-wall carbon nanotubes (MWCNT) 20 nm in diameter and 1-4 mm long are difficult to manipulate freely because of the high length to diameter aspect ratio of 100,000:1. Therefore, nanotube bundles about 1 µm diameter and containing thousands of MWCNT were used for welding to the tungsten probe. First, the nanotube array up to 1 mm was peeled off the Si substrate and laid down on an aluminum sheet. A smaller bundle of nanotubes was attached to the tungsten probe by applying a potential of about 1 V between the aluminum block and the tungsten probe, in air. Then a bare tungsten probe and the nanotube loaded tungsten probe were aligned at the edge of tungsten probe, as shown in Figure 2a. Then high potential up to 5V was applied which welded the nanotube bundle to the tungsten probe (Figure 2b). The tungsten probe was moved backward until the right hand tungsten probe loses contact with the nanotube. Finally, Figure 2f shows the welded nanotube bundle on the tungsten probe. When working with the mm long nanotubes, it becomes apparent that the aspect ratio of the individual nanotubes is so large that individual nanotubes easily deflect and bend and may not support their own weight, and thus cannot be easily manipulated. The self-assembly growth process to form long arrays and working with arrays and bundles of nanotubes allows manufacturing of larger and

stronger probes. The bundle of nanotubes on the probe may be further sharpened using acid etching or electrical discharge. The welding process needs further investigation to improve the consistency of the weld strength and later will be done in an inert atmosphere.

After welding nanotube bundle on tungsten needle, there are two approaches to insulating the nanotube bundle and tungsten needle. In the first approach, a UV-hardening polymer was applied to electrically insulate the tungsten part of the needle and expose only the nanotube part in the analyte. The UV-Curing polymer was coated on the tungsten needle under the microscope, and the procedure was repeated five times to ensure complete insulation [11]. Then the coated needle is cured under the UV lamp for one-half hour. The final coated needle is shown in Figure 3.

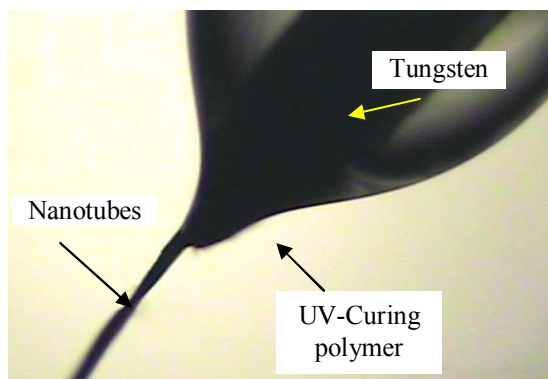


Figure 3. Nanotube bundle on the tungsten probe (a) and on the insulated tungsten probe (b)

In the second approach, the nanotube bundle and tungsten needle was placed in a glass tube and sealed with the UV curable polymer to strengthen and allow handling of the needle sensor. A schematic of the needle design is shown in Figure 4. Important steps in the process are welding the nanotubes to the needle to reduce the contact resistance, and coating the nanotubes to expose only the tips. Measured contact resistance was typically from 1 K Ω to 100 K Ω . Reducing the contact resistance is a subject of continuing work.

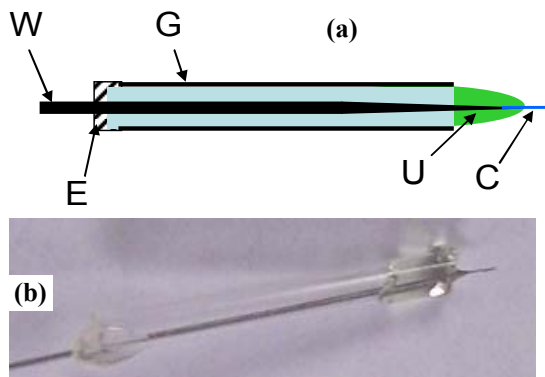


Figure 4. Schematic of a nanotube needle electrode: (a) W, tungsten needle ; E, epoxy; G, glass tube; U, UV curing agent; C, carbon nanotube bundle; and (b) the final nanotube probe electrode

III. RESULTS

In order to evaluate the electrochemical properties of the CNT electrode, cyclic voltammetry (CV) was carried out using a Bioanalytical Systems (BAS, West Lafayette, IN) electrochemical analyzer operated by an Epsilon software system and with a C3 cell stand in a Faraday cage. A platinum wire and a Ag/AgCl wire were used as the auxiliary and reference electrodes, respectively. All reagents ($K_3Fe(CN)_6$ (Fisher, 99%), and KNO_3 (Fisher, 99%) were prepared fresh daily in deionized water.

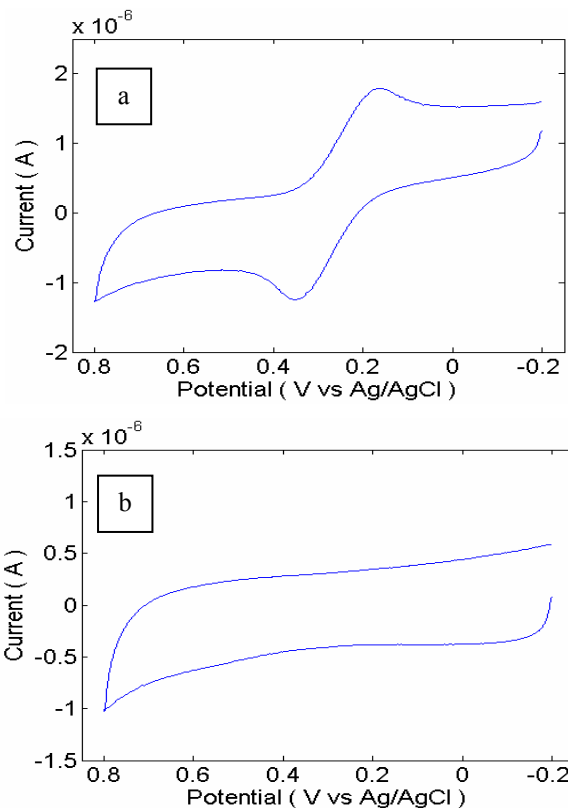


Fig. 5. Cyclic voltammetry of a nanotube needle electrode in a supporting electrolyte 1.0 M KNO_3 for two conditions: (a) with a 6 mM $K_3Fe(CN)_6$ redox probe; and (b) without the redox probe. Both conditions are at a 100 mV/s scan rate.

In performing the sensor experiments, each experiment was repeated several times and only the nanotube end is exposed to the analyte. Because $Fe(CN)_6^{3-/4-}$ is useful for probing nanotube electrode kinetics, cyclic voltammetry (CV) for the respective reduction of 6 mM $K_3Fe(CN)_6$ in a 1.0 M KNO_3 was performed to examine the redox behavior of the nanotube needle electrodes. As shown in Figure 5, a sigmoidal-shaped voltammogram was observed with 100 mV/s scan rate, indicating that the mass transport was dominated by radial diffusion. The cyclic voltammetric peak-separation (ΔE_p) of $Fe(CN)_6^{3-/4-}$ at 100 mV/s is approximately 120 mV, suggesting fast electron transfer. Radial diffusion of the nanotube tower electrode gives rise to several advantages over macroelectrodes. As shown in Figure 5(b), the background voltammograms show typical interfacial capacitance. Probably, opening the ends or etching the nanotube array to expose the

edge plane might decrease the capacitance and the electron transfer resistance. This concept requires further study.

Amperometric testing with different concentration of hydrogen peroxide (Sigma-Aldrich) was done in a phosphate buffer solution (pH 7.4). A glucose oxidase (Sigma-Aldrich) solution was coated on the nanotube electrode and left for 2 hours. The glucose oxidase was then coated with a semi-permeable membrane using Nafion (Dupont). Glucose (Sigma-Aldrich) at different concentrations was detected in a phosphate buffer solution using the enzyme-modified nanotube needle electrode.

Figure 6 shows the amperometric response from the nanotube needle electrode at an applied potential of 0.5 V due to the successive addition of 0.5 mM and 1 mM H₂O₂ in Phosphate Buffer Solution with a pH 7.4 in the stirred solution. The result shows that a well defined current response for the glucose is obtained. In particular, the response current increases immediately after each addition of 0.5 mM of hydrogen peroxide solution, as indicated by the arrows. The stability of the biosensor is another critical factor for commercial applications. In particular, long-term stability is needed for biosensor development. In this experiment, the response generated a steady-state current signal for more than 100 seconds.

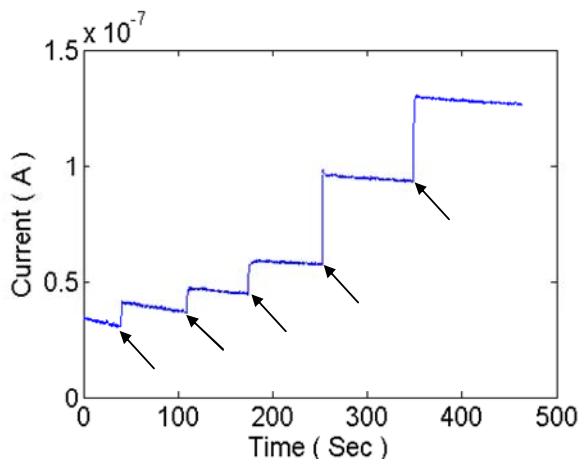


Figure 6. The amperometric response of a nanotube needle electrode sensor at an applied potential of 0.5V versus the Ag/AgCl reference electrode due to the successive addition of 0.5 and 1 mM H₂O₂ in PBS (pH 7.4) at room temperature.

Figure 7 shows the amperometric response of the biosensor in which 0.2 mM glucose is added at each step at a potential of 0.5 V in PBS (pH 7.4). Even though there is slight noise in the signal, the current response increases immediately after each addition of 0.2 mM of glucose in the PBS solution. This change in response is repeated and keeps the same value for 100 seconds. This good sensitivity and stability are an advantage of the nanotube-needle biosensor. The good stability is probably because of the structure of the nanotube needle electrode which provides a large surface area to immobilize the GOx and maintain this high activity. At the same time, the nanotube

needle electrode may promote electron transfer in the bioelectrochemical reaction.

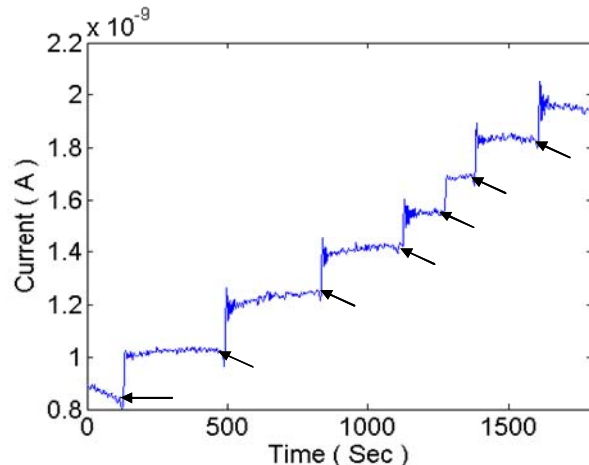


Figure 7. The amperometric response at an applied potential of 0.55 V versus the Ag/AgCl reference electrode from the nanotube needle sensor due to the successive addition of 0.2 mM glucose in a phosphate buffer solution (pH 7.4) at room temperature

IV. RESULTS/DISCUSSION

The needle electronic biosensor has good sensitivity which can be improved as the nanotube tip is sharpened. Applications for the biosensor include cancer detection, monitoring bone markers, and glucose sensing.

REFERENCES

- [1] L. C. Clark, and C. Lyons, *Ann. N. Y. Acad. Sci.*, 114, 653-662 (1962).
- [2] J. Wang, and M. Musameh, *Anal. Chem.* 75, 2075-2079 (2003).
- [3] Y. Lin, F. Lu, Y. Tu, and Z. Ren, *Nano Letters*, 4(2), 191-195 (2004).
- [4] Y.H. Yun, V. Shanov, M.J. Schulz, Z. Dong, A. Jazieh, W.R. Heineman, H. B. Halsall, D. K.Y. Wong, A. Bange, Y. Tu, S. Subramaniam, *Sensors and Actuators B*, in press.
- [5] Y.H. Yun, R. Gollapudi, V. Shanov, M. J. Schulz, Z. Dong, A. Jazieh, W.R. Heineman, B. Halsall, D.K.Y. Wong, Y. Tu, S. Subramaniam, *Journal of Nanoscience & Nanotechnology*, in press.
- [6] J. Li, H. T. Ng, A. Cassell, W. Fan, H. Chen, Q. Ye, J. Koehne, J. Han, and M. Meyyappan, *Nano letters*, 3(5), 597-602 (2003).
- [7] J.H. Hafner, C. L. Cheung, A.T. Woolley, C.M. Lieber, *Progress in Biophysics and Molecular Biology*, 77, 73-110 (2001).
- [8] J. H. Hafner, C. L. Cheung, C.M. Lieber, *Nature*, 398, 761-762 (1999).
- [9] Y.H. Yun, V.N. Shanov, Y. Tu, and M.J. Schulz, *Smart Materials and Structures* in Review.
- [10] Y.H. Yun, V. Shanov, Y. Tu, S. Subramaniamb, M.J. Schulz, *Journal of chemical Physics B*, in Review.
- [11] H. Boo, R.A. Jeong, S. Park, K. Kim, K.H. An, Y.H. Lee, J.H. Han, H.C. Kim, and T.D. Chung, 78, 617-620 (2006).
- [12] Z.W. Pan, S.S. Xie, L. Lu, B.H. Chang, L.F. Sun, W.Y. Zhou, G. Wang, and D.L. Zhang, *Applied physics letters*, 74(21), 3152 (1999).